On the Dynamic Analysis of Curved and Twisted Cylinders Transporting Fluids

R. W. DOLL

TRW Systems Group,
Redondo Beach, Calif.

C. D. MOTE, JR.

Depart. of Mechanical Engineering,
University of California,
Berkeley, Calif.

The longitudinal, torsional and 2-transverse equations of motion are formulated for the titled problem through application of Hamilton's Principle. Curvature-torsion conditions under which linear oscillation in a plane can exist are identified. The finite element method with isoparametric elements is used for discretization prior to spectra analysis. Natural frequency calculations over a range of mass transport velocities and cylinder end conditions were carried out for comparison with constant and variable curvature analyses and experiment. These results support the application of the constant curvature, inextensible centerline model for curved cylinder vibration analysis.

Introduction

The transverse vibration and stability of cylinders transporting fluids has been extensively studied during the last quarter century. For a review of the related literature the reader is referred to references [1–7, 19].[1] Research efforts have concentrated on the linear theoretical relationship between the mass transport velocity and the straight conduit transverse natural frequencies. Relatively little attention has been directed to curved cylinders although Unny, et al. [3] and Chen [4, 5] derived the in-plane (in the plane of principal curvature) and the out-of-plane equations of motion. In these formulations the assumption of an inextensible centerline permitted a reduction in the number of equations by one. The curvature and length of the cylinder symmetry axis were constant and independent of the transport velocity. Recently Hill and Davis [6] introduced the influence of initial, flow dependent, membrane tension on the curved cylinder natural frequencies. They concluded that the natural frequency-transport velocity relationship was sufficiently sensitive to initial, membrane stresses that the previous analyses were conceptually and numerically incorrect. Experimental verification of the models has not kept pace with the theoretical developments. This is unfortunate because the cylinder transporting a mass in slug flow theoretical model is essentially a planer Euler-Bernoulli beam formulation and is not so obviously correct that it should be accepted without question.

The theoretical studies herein were stimulated by an experimental investigation of the natural frequencies of straight and "almost" straight cylinders [7]. In that study the observed natural frequency-mass transport velocity relationship deviated from the straight cylinder theory at the higher velocities without quantitative explanation. It was suspected that small curvature of the symmetry axis was responsible for the discrepancies between theory and observation. Also the response was never in the plane of the excitation but the orbit of a point on the symmetry axis was approximately elliptical. In this paper the longitudinal, torsional and transverse equations of motion are formulated for a curved and twisted rod transporting mass in slug flow at constant velocity. The kinematics of the rod are derived in Frenet-Serret curvature-torsion parameters, and the rod-conduit equations of motion are obtained from the extended Hamilton's Principle. Special attention is given to the identification of curvature-torsion conditions under which response in the plane and normal to the plane of the excitation is expected. The finite element method with isoparametric elements is used for discretization of the equations of motion prior to spectral analysis. The numerical procedures developed simulate both the constant curvature and variable curvature cylinder models mentioned. Both theoretical models are tested against experimental data [7] for small curvature cylinders. The constant curvature algorithm predicts a natural frequency-transport velocity relationship which more closely approximates the experimental observations.

Theory

The physical model is a long, hollow, prismatic rod transporting a continuous mass along its centerline. The rod cross-section displacement is a function of the centerline or longitudinal coordinate s which reduces the kinematics of the rod to those of a one-dimensional space curve following Love [8] and Tso [9]. The rod centerline displacement may not be small although strains are assumed small. Rotary inertia caused by bending, transverse shearing deformations and anticlastic deformation are not included.

The curvatures of the x and y principal centroidal axes are κ_0 and κ_0', and τ_0 is the torsion as shown in Fig. 1(a). The resultant curvature at point 0 is seen to be

[1] Numbers in brackets designate References at end of paper.

Contributed by the Pressure Vessels and Piping Division and presented at the Second National Congress on Pressure Vessels and Piping, San Francisco, Calif., June 23–27, 1975, of THE AMERICAN SOCIETY OF MECHANICAL ENGINEERS. Manuscript received at ASME Headquarters, July 30, 1975.

$$\kappa_0^* = \sqrt{\kappa_0^2 + \kappa_0'^2} = 1/R \tag{1}$$

with

$$\kappa_0'/\kappa_0 = \tan \nu \tag{2}$$

The curvature-torsion parameters are a function of position s as shown in Fig. 1(*b*), and the coordinates acquire prime superscripts in the deformed state. The coordinate system ($\underset{\sim}{e}_1$, $\underset{\sim}{e}_2$, $\underset{\sim}{e}_3$) is inertial; the system ($\underset{\sim}{e}_1^{(0)}$, $\underset{\sim}{e}_2^{(0)}$, $\underset{\sim}{e}_3^{(0)}$) is the principal system at point P_0; the system ($e_n^{(0)}$, $e_b^{(0)}$, $e_t^{(0)}$) is the normal-binormal-tangential system at point P_0. The relationship between the rod displacements w, u, v, θ and the curvature-torsion is developed from curvature-torsion definitions and the defined coordinate systems. Following some manipulations [10] one obtains

$$\begin{aligned}\kappa_1 = {} & \kappa_0 - v_{,ss} - (\tau_0 u)_{,s} + (\kappa_0 w)_{,s} + \kappa_0'\theta \\ & - \tau_0 u_{,s} + \tau_0^2 v - \kappa_0'\tau_0 w - \kappa_0' u_{,s} v_{,s} \\ & - u_{,s}\theta_{,s} - \tau_0 v_{,s}\theta + \kappa_0 v_{,s}^2 \end{aligned} \tag{3}$$

$$\begin{aligned}\kappa_1' = {} & \kappa_0' + u_{,ss} - (\tau_0 v)_{,s} + (\kappa_0' w)_{,s} - \tau_0 v_{,s} \\ & + \tau_0^2 u + \kappa_0 \tau_0 w - \kappa_0 \theta + v_{,ss}\theta + (\tau_0 u)_{,s}\theta \\ & + \tau_0 u_{,s}\theta + \kappa_0' u_{,s}^2 - \kappa_0 u_{,s} v_{,s} \end{aligned} \tag{4}$$

$$\begin{aligned}\tau_1 = {} & \tau_0 + \tau_0\kappa_0' u + \kappa_0 u_{,s} - \kappa_0 \tau_0 v + \kappa_0' v_{,s} \\ & + \theta_{,s} + \tau_0\theta^2 + \kappa_0' u_{,s}\theta - \kappa_0 v_{,s}\theta + \tau_0 u_{,ss} u + u_{,ss} v_{,s} \end{aligned} \tag{5}$$

The displacements w, u, v, θ are illustrated in Fig. 1(*a*, *b*). The development of equations (3)–(5) follows that found in Love [8], and they reduce to results found therein when κ_0 and all nonlinear terms are deleted. The writers are unaware of an earlier derivation of these relationships.

The correct statement of Hamilton's Principle for mass transport systems, attributed to Benjamin [11], is

$$\delta I = \delta \int_{t_1}^{t_2} L dt - \int_{t_1}^{t_2} m_f c(\dot{\underset{\sim}{r}} + \underset{\sim}{c}) \cdot \delta \underset{\sim}{r} \Big|_{s=l_0}^{s=l_1} dt = 0 \tag{6}$$

where the Lagrangian L is the kinetic minus the potential energy of the rod plus fluid or transport mass, m_f is the fluid mass/length, $\underset{\sim}{c}$ is the mean transport velocity relative to the rod, c is the magnitude of mean transport velocity vector, $\underset{\sim}{r}$ is the inertial centerline position, and the rod extends from $s = l_0$ to $s = l_1$.

The rod position and velocity are

$$\underset{\sim}{r} = \underset{\sim}{r}_0 + \underset{\sim}{u} \tag{7}$$

$$\dot{\underset{\sim}{r}} = u_{,t}\underset{\sim}{e}_1^{(0)} + v_{,t}\underset{\sim}{e}_2^{(0)} + w_{,t}\underset{\sim}{e}_3^{(0)} \tag{8}$$

and the rotation gives

$$\dot{\underset{\sim}{\theta}} = \theta_{,t}\underset{\sim}{e}_3^{(0)} \tag{9}$$

The fluid absolute velocity is determined from its position denoted by $\underset{\sim}{r}'$

$$\dot{\underset{\sim}{r}}' = \dot{\underset{\sim}{r}}_0 + \dot{\underset{\sim}{u}} + c \tag{10}$$

The inertial velocity becomes

$$\dot{\underset{\sim}{r}}' = \dot{\underset{\sim}{u}} + \underset{\sim}{c} = \dot{\underset{\sim}{u}} + c\underset{\sim}{e}_3'^{(0)} \tag{11}$$

and in the undeformed coordinates

$$\begin{aligned}\dot{\underset{\sim}{r}}' = {} & [u_{,t} + c(u_{,s} - \tau_0 v + \kappa_0' w)]\underset{\sim}{e}_1^{(0)} \\ & + [v_{,t} + c(v_{,s} + \tau_0 u - \kappa_0 w)]\underset{\sim}{e}_2^{(0)} \\ & + [w_{,t} + c]\underset{\sim}{e}_3^{(0)} \end{aligned} \tag{12}$$

The kinetic energy of the system is obtained by substitution into

$$T = \tfrac{1}{2} \int_{l_0}^{l_1} \{m_c \dot{\underset{\sim}{r}} \cdot \dot{\underset{\sim}{r}} + I\dot{\underset{\sim}{\theta}} \cdot \dot{\underset{\sim}{\theta}} + m_f \dot{\underset{\sim}{r}}' \cdot \dot{\underset{\sim}{r}}'\} ds \tag{13}$$

where m_c is the rod mass/length and I is inertia/length. The potential energy of the incompressible transport mass is zero, and the potential energy of the rod is determined from classical beam theory for bending, torsion and tension;

$$\frac{M_{11}}{EI_1} = \kappa_1 - \kappa_0 \tag{14}$$

$$\frac{M_{22}}{EI_2} = \kappa_1' - \kappa_0' \tag{15}$$

$$\frac{M_{33}}{GJ} = \tau_1 - \tau_0 \tag{16}$$

$$\frac{F_{33}}{AE} = \epsilon_{33} \tag{17}$$

The curvature-torsion terms are given in (3)–(5), and ϵ_{33} is the

Nomenclature

A = area
$\underset{\sim}{c}$ = relative fluid transport velocity
c = fluid transport velocity
$\underline{C}$ = dissipation matrix
ds = differential segment of rod in unstressed state
D^k = differential operator $\partial^k(\ )/\partial s^k$
e = h/l_0, eccentricity
E = modulus of elasticity
F_{33} = axial force
G = shear modulus
h = cylinder centerline deviation at midpoint—Fig. 4
I = polar moment of inertia per unit length
I_1 = x-axis second moment of area
I_2 = y-axis second moment of area
J = polar moment of area
$\underline{K}$ = stiffness matrix
l_0 = arc length
m_c = cylindrical mass per unit length
m_f = fluid mass per unit length
$\underline{M}_{ii}$ = moments
M = lumped inertia matrix
N = total number of elements
R = radius of centerline curvature
$\underset{\sim}{r}$ = centerline position in the stressed configuration
$\underset{\sim}{r}_0$ = centerline position in the unstressed configuration
s = centerline coordinate
$u(\eta, t)$ = relative displacement with components w, u, v, θ
u = generalized coordinate along the normal
v = generalized coordinate along the binormal
$\mathbf{v}'^{(e)}(t)$ = local nodal point vector
$\mathbf{v}^{(e)}(t)$ = global nodal point vector
w = generalized coordinate along the tangent
α_i = transformation angle in Fig. 2
$\underline{\alpha}$ = inertia matrix
$\underline{\beta}$ = dissipation matrix
$\underline{\gamma}$ = stiffness matrix
γ_i = transformation angle in Fig. 2
ϵ_{33} = finite strain
η = dimensionless curvilinear coordinate
θ = rotation coordinate
κ_0^* = principal intial curvature
κ_0 = x-axis principal initial curvature component
κ_0' = y-axis principal initial curvature component
κ_1 = final curvature component about x-axis
κ_1' = final curvature component about y-axis
λ = complex natural frequency
ν = angle between κ_0 and κ_0^* in the initial configuration
τ_0 = initial torsion
τ_1 = final torsion
$\Phi^{(e)}(\eta)$ = interpolation functions
$(\ )^e$ = quantity defined for each element

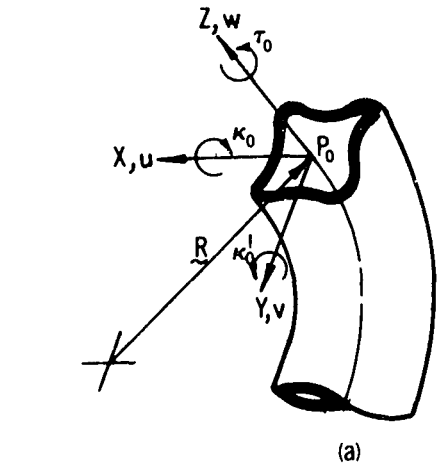

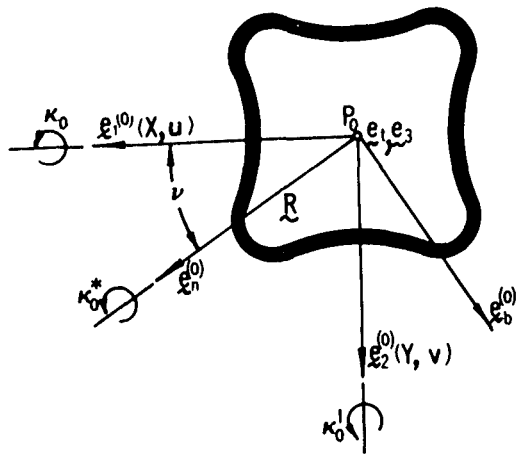

Fig. 1(a) Curvature-torsion parameters for the principal axes

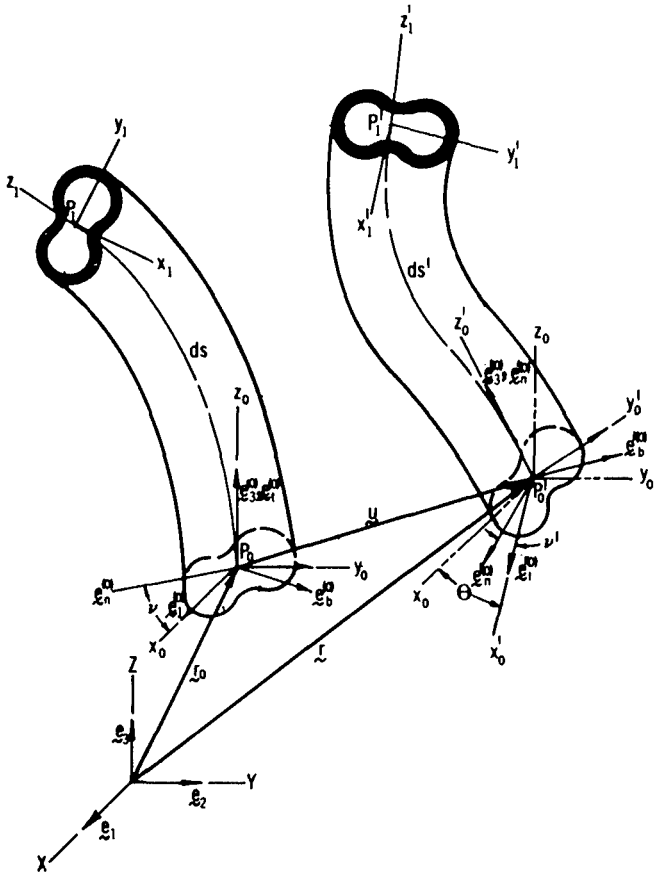

(a) UNDEFORMED (b) DEFORMED

Fig. 1(b) Deflection of a curved and twisted rod element

finite strain for small strain and moderate to large rotations;

$$\epsilon_{33} = e_{33} + {}^1/_2(\omega_{23}^2 + \omega_{13}^2) \tag{18}$$

The axial strain becomes upon calculation

$$\epsilon_{33} = (w_{,s} - \kappa_0' u + \kappa_0 v) + {}^1/_2[(u_{,s} - \tau_0 v + \kappa_0' w)^2 + (v_{,s} - \kappa_0 w + \tau_0 u)^2] \tag{19}$$

The centerline deformation is small but not zero. The total potential energy becomes then

$$V = {}^1/_2 \int_{t_0}^{t_1} \{M_{11}(\kappa_1 - \kappa_0) + M_{23}(\kappa_1' - \kappa_0') + M_{33}(\tau_1 - \tau_0) + F_{33}\epsilon_{33}\} ds \tag{20}$$

The extended Hamilton's Principle (6) can now be formulated by substitution. From the linearized (3)–(5), the stationary principle (6) gives

$$\begin{aligned}
\delta I_h = \int_{t_1}^{t_2} \Bigg[& \delta \left\{ {}^1/_2 \int_{t_0}^{t_1} m_c[u_{,t}^2 + v_{,t}^2 + w_{,t}^2] + I\theta_{,t}^2 \right\} \Bigg] ds \\
& + {}^1/_2 \int_{t_0}^{t_1} m_f[(u_{,t} + c(u_{,s} - \tau_0 v + \kappa_0' w))^2 \\
& + (v_{,t} + c(v_{,s} + \tau_0 u - \kappa_0 w))^2 + (w_{,t} + c)^2] ds \\
& - {}^1/_2 \int_{t_0}^{t_1} EI_1[-v_{,ss} - (\tau_0 u)_{,s} + (\kappa_0 w)_{,s} - \tau_0 u_{,s} \\
& + \tau_0^2 v - \kappa_0' \tau_0 w + \kappa_0' \theta]^2 ds \\
& - {}^1/_2 \int_{t_0}^{t_1} EI_2[u_{,ss} - (\tau_0 v)_{,s} + (\kappa_0' w)_{,s} - \tau_0 v_{,s} \\
& - \tau_0^2 u + \kappa_0 \tau_0 w - \kappa_0 \theta]^2 ds \\
& - {}^1/_2 \int_{t_0}^{t_1} GJ[\theta_{,s} + \kappa_0 u_{,s} + \kappa_0' v_{,s} + \kappa_0' \tau_0 u - \kappa_0 \tau_0 v]^2 ds \\
& - {}^1/_2 \int_{t_0}^{t_1} AE[w_{,s} - \kappa_0' u + \kappa_0 v]^2 ds \Bigg\} \\
& - m_f c\{[u_{,t} + c(u_{,s} - \tau_0 v + \kappa_0' w)]\delta u \\
& + [v_{,t} + c(v_{,s} + \tau_0 u - \kappa_0 w)]\delta v \\
& + [c + w_{,t}]\delta w\} \Big|_{s=t_0}^{s=t_1} \Bigg] dt = 0
\end{aligned} \tag{21}$$

Some discussion of the nonlinear formulation can be found in [10] but the problem size and complexity quickly become unmanageable and unwarranted at this time. It will not be pursued here. The Euler equations obtained from (21) in a straightforward but lengthy manner are

$$\underset{\sim}{\alpha}\ddot{\underset{\sim}{x}} + \underset{\sim}{\beta}\dot{\underset{\sim}{x}} + \underset{\sim}{\gamma}\underset{\sim}{x} = \underset{\sim}{0} \tag{22}$$

where the 4×4 $\underset{\sim}{\alpha}$, $\underset{\sim}{\beta}$ and $\underset{\sim}{\gamma}$ are given in Appendix 1, $\underset{\sim}{x}^T = [w, u, v, \theta]$ and the boundary conditions are given in Table 1. These

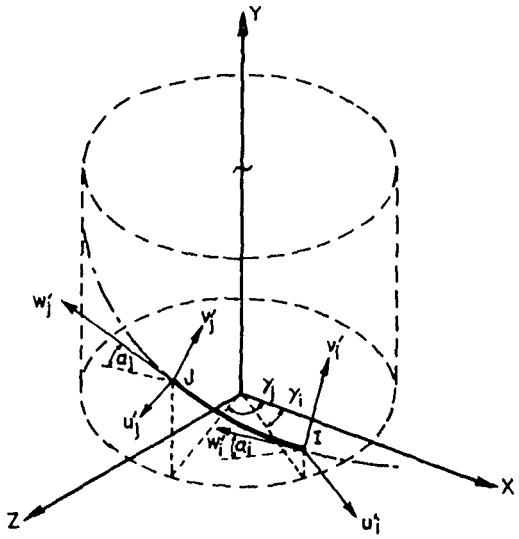

Fig. 2 Finite element for the curved and twisted cylinder

equations are not in the literature, but they reduce to available formulations for curved rods and tubes. If c, κ_0, $\kappa_{0,s}$, $\kappa_0'_{,s}$ and $\tau_{0,s}$ vanish, then they reduce to those found in Tso [9] for curved and twisted rods. The equations of Chen [5] are obtained by equating κ_0, τ_0, $\kappa_{0,s}$, $\kappa_{0,s}'$ and $\tau_{0,s}$ to zero, by equating s to $R\theta$, $\kappa_0' = 1/R$ and by employing the inextensible centerline hypothesis $u = \partial w/\partial\theta$. The perturbation equations of Hill and Davis [6] can not be obtained by reduction of these equations. Terms arise in [6] that are not present here.

Rod geometries under which coupled in-plane and out-of-plane response occurs (coupled u, v) are determined from the (2, 3) and (3, 2) coefficients of equation (22). A nonvanishing coefficient insures coupled motion. In summary, coupled response results for the following rods:

(a) If the rod is initially straight but twisted, coupled response occurs. Here, $\kappa_0 = \kappa_0' = 0$, $\tau_0 \neq 0$ and the coefficients of (22) are

$$\underline{\beta} = \begin{bmatrix} 0 & 0 & 0 & 0 \\ 0 & \beta_{22} & \beta_{23} & 0 \\ 0 & -\beta_{23} & \beta_{33} & 0 \\ 0 & 0 & 0 & 0 \end{bmatrix} \quad \underline{\gamma} = \begin{bmatrix} \gamma_{11} & 0 & 0 & 0 \\ 0 & \gamma_{22} & \gamma_{23} & 0 \\ 0 & -\gamma_{23} & \gamma_{33} & 0 \\ 0 & 0 & 0 & \gamma_{44} \end{bmatrix}$$

indicating coupling of the flexural displacements u, v and no coupling of w, θ.

(b) If the rod is not twisted and if the principal radius of curvature is not aligned with a rod cross-section principal axis, total coupling of all variables occurs. Here $\kappa_0 \neq 0$, $\kappa_0' \neq 0$ and $\tau_0 = 0$.

(c) If the rod is initially curved and twisted, coupling of all variables occurs. Here $\kappa_0 \neq 0$ and/or $\kappa' \neq 0$, $\tau_0 \neq 0$.

It is interesting to note that the mass transport velocity c does not create the coupled motion through the introduction of additional coupling terms. The velocity merely modifies existing coupled problems. Uncoupled response occurs for the following rods:

(a) If the rod is straight and not twisted, then all dependent variables are uncoupled. Here $\kappa_0 = \kappa_0' = \tau_0 = 0$.

(b) If the rod is not twisted and its radius of curvature is along a cross-section principal axis, then the in-plane and out-of-plane responses are uncoupled. Here $\kappa_0 = 0$ or $\kappa_0' = 0$, $\tau_0 = 0$. Coupled motion occurs within each plane. Note that the nonvanishing curvature need not be constant for uncoupling of the in- and out-of-plane response to occur.

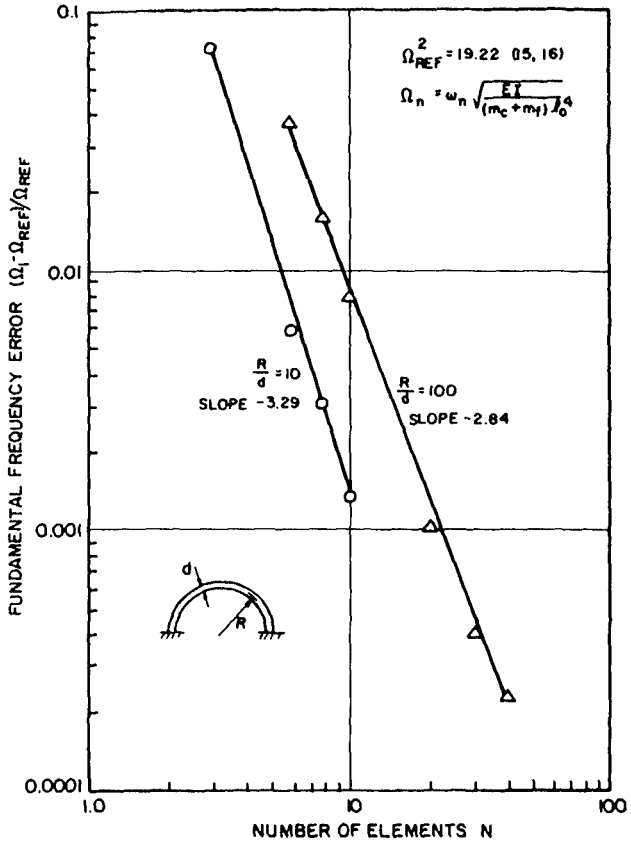

Fig. 3 Convergence of finite element for semi-circular ring sector

Numerical Analysis

The class of problems analyzed numerically is selected for comparisons with available literature. For the remainder of the paper the rod is a hollow, circular cylinder with curvature in a plane. Then

$$\kappa_0 = 0 \tag{23}$$

$$\kappa_0' = \kappa_0^* \tag{24}$$

$$\tau_0 = 0 \tag{25}$$

and uncoupled in-plane and out-of-plane oscillation is possible. Note that the inextensible centerline hypothesis has not been used.

The finite element discretization of equation (21) following substitution of equations (23)–(25) divides the cylinder into N elements illustrated in Fig. 2. The local field variable is

$$\underline{u}^{(e)}(\eta, \tau) = \underline{\Phi}^{(e)}(\eta)\mathbf{v}^{(e)}(\tau) \tag{26}$$

where the nodal coefficients are

$$\mathbf{v}^{(e)T} = [w_i', u_i', v_i', \theta_i', w_{i,s}, \ldots, \theta_{i,s}, w_j', \ldots, w_{j,s}', \ldots, \theta_{j,s}'] \tag{27}$$

and the nonzero Hermite interpolation polynomials on $-1 \leqq \eta \leqq +1$ are

$$\begin{aligned} \Phi_{KK}{}^{(e)} &= (2 - 3\eta + \eta^3)/4 \\ \Phi_{K(K+4)}{}^{(e)} &= (1 - \eta - \eta^2 + \eta^3)/8 \\ \Phi_{K(K+8)}{}^{(e)} &= (2 + 3\eta - \eta^3)/4 \\ \Phi_{K(K+12)}{}^{(e)} &= (-1 - \eta + \eta^2 + \eta^3)/8 \end{aligned} \tag{28}$$

where $K = 1, 2, 3, 4$. The local x, y, z, θ are similarly distributed. The discretization follows directly with a few points worthy of

comment. The interpolation (28) uses the curvilinear coordinate η and the curvature-torsion parameters in equation (21) are defined in terms of s. The derivatives

$$\frac{\partial \eta}{\partial s} = \left[\left(\frac{\partial x}{\partial \eta} \right)^2 + \left(\frac{\partial y}{\partial \eta} \right)^2 + \left(\frac{\partial z}{\partial \eta} \right)^2 \right]^{-1/2} \quad (29)$$

$$\frac{\partial^2 \eta}{\partial s^2} = -\left(\frac{\partial \eta}{\partial s} \right)^4 \left[\frac{\partial x}{\partial \eta} \frac{\partial^2 x}{\partial \eta^2} + \frac{\partial y}{\partial \eta} \frac{\partial^2 y}{\partial \eta^2} + \frac{\partial z}{\partial \eta} \frac{\partial^2 z}{\partial \eta^2} \right] \quad (30)$$

$$\frac{\partial^3 \eta}{\partial s^3} = -4\left(\frac{\partial s}{\partial \eta} \right) \frac{\partial^2 \eta}{\partial s^2} - \left(\frac{\partial \eta}{\partial s} \right)^5 \left[\left(\frac{\partial^2 x}{\partial \eta^2} \right)^2 + \left(\frac{\partial^2 y}{\partial \eta^2} \right)^2 + \left(\frac{\partial^2 z}{\partial \eta^2} \right)^2 + \frac{\partial x}{\partial \eta} \frac{\partial^3 x}{\partial \eta^3} + \frac{\partial y}{\partial \eta} \frac{\partial^3 y}{\partial \eta^3} + \frac{\partial z}{\partial \eta} \frac{\partial^3 z}{\partial \eta^3} \right] \quad (31)$$

and the curvature-torsion parameters

$$\kappa_0' = -\left[\left(\frac{\partial^2 x}{\partial s^2} \right)^2 + \left(\frac{\partial^2 y}{\partial s^2} \right)^2 + \left(\frac{\partial^2 z}{\partial s^2} \right)^2 \right]^{1/2} \quad (32)$$

$$\tau_0 = \frac{1}{\kappa_0'^2} \begin{vmatrix} \frac{\partial x}{\partial s} & \frac{\partial y}{\partial s} & \frac{\partial z}{\partial s} \\ \frac{\partial^2 x}{\partial s^2} & \frac{\partial^2 y}{\partial s^2} & \frac{\partial^2 z}{\partial s^2} \\ \frac{\partial^3 x}{\partial s^3} & \frac{\partial^3 y}{\partial s^3} & \frac{\partial^3 z}{\partial s^3} \end{vmatrix} \quad (33)$$

are required for the necessary coordinate transformation. A second point is that the local coordinates in which the stiffness is formulated must be rotated into the global coordinate system during assembling of the equations. An α-rotation shown in Fig. 2 is followed by a γ-rotation for all points I and J. And finally, a lumped inertia basis is used for w, u, v and θ [12].

If the rod curvature is assumed constant for all c, then κ_0' in equation (24) is constant as in [3–5]. When the rod equilibrium curvature is a function of fluid velocity c, then κ_0' in equation (24) is the $c = 0$ curvature as in [6] and $\kappa_{0,s}'$ terms are retained in equation (21). The numerical procedure for computing curvature variations is outlined as follows. The cylinder has an initial curvature (24) at $c = 0$. For a small velocity increment the normal acceleration of the fluid displaces the cylinder. The equations are then reformulated in the new configuration, and the velocity is incremented again. At velocity intervals the eigenvalue calculation is carried out for the desired natural frequency-transport velocity relationship.

The stationarity of the discretized functional (21) leads to the discrete equations of motion

$$\underline{M}\ddot{\underline{v}} + \underline{C}\dot{\underline{v}} + \underline{K}\underline{v} = \underline{0} \quad (34)$$

where $\underline{M}$ is diagonal and $\underline{C}$ and $\underline{K}$ are unsymmetric. The eigenvalue problem becomes

$$\begin{bmatrix} -\underline{K}^{-1}\underline{C} & -\underline{K}^{-1}\underline{M} \\ \underline{I} & \underline{0} \end{bmatrix} \begin{Bmatrix} \underline{V} \\ \underline{W} \end{Bmatrix} = \frac{1}{\lambda} \begin{Bmatrix} \underline{V} \\ \underline{W} \end{Bmatrix} \quad (35)$$

where

$$\underline{V} = \underline{v} \exp(\lambda \tau)$$
$$\underline{W} = \lambda \underline{V} \quad (36)$$

The eigenvalue problem (35) was solved by a reduction to upper Hessenberg form and utilization of the QR algorithm.

Results

For a third order interpolation Fried [13] has shown that in the limit the mean rate of convergence is N^{-4} where N = no. of elements. The convergence rate decreases as element distortion increases to a lower bound of N^{-2}. Sabir [14] shows that the convergence decreases as the relative thickness (R/d) decreases and/or the included angle increases. The convergence of the present analysis is tested against exact solutions for two clamped semi-circular rings [15, 16] in Fig. 3. The convergence is satisfactory and consistent with expectations.

The in-plane natural frequency as a function of eccentricity $e = h/l_0$ is computed for a ring of length l_0 between clamped ends; see Fig. 4. The fundamental frequency relative error is 0.0128 percent for the straight rod, and approximately 1 percent [4] for the semi-circular rod with a six element model. The latter reference values are obtained from a published curve so error evaluation is of limited accuracy. Also the two theoretical models are not identical as mentioned. The odd vibration modes (even number of interior nodes), and especially the fundamental mode, are sensitive to eccentricity for small e. The "1/2 sine" mode disappears with increasing e. A similar observation is made with pinned end conditions. The approach and separation of the modes 1 and 3 loci *may* be an example of the curve-veering phenomenon discussed recently by A. W. Liessa [17]. He postulates that discretization errors in the transition (loci crossing) regions may cause the loci to veer abruptly where the exact solution would cross if it were known. The problem cannot be eliminated by a more refined discretization. The error, if it exists, is confined to the transition region.

The analysis of out-of-plane vibrations shows no odd-mode sensitivity to e, and the influence of e is similar to that observed for modes 2 and 4 in Fig. 4. For large e the frequency decreases because of increased cylinder length.

The in- and out-of-plane fundamental frequencies of a cylinder curved into a 180-deg arc are analyzed for comparison of the formulation with current literature. The geometry and mass transport particulars are radii of curvature and gyration ratio $R/a = 40$, $m_c = m_f$, $R/d = 15.1$, and a six element model is analyzed. For the configuration (23)–(25), the in- and out-of-plane responses are uncoupled and shown in Fig. 5. The constant curvature results compare well to those of Chen [4, 5]. Since the formulation here permits centerline extension whereas that of Chen does not, these results support the inextensible centerline hypothesis for this geometry. Allowance of curvature variations with increasing transport velocity influences natural frequencies through two mechanisms. First the induced membrane stress increases the natural frequencies, and second the change in curvature of cylinder geometry shifts the natural frequencies as illustrated in Fig. 4. The correspondence between these results and those of Hill and Davis [6] is also reasonably good. For a simply supported cylinder the results show a similarly satisfactory comparison.

The analysis has also been applied to cantilevered semi-circular cylinders and they experience flutter instability as observed previously [1, 18].

No vibration data on highly curved cylinders transporting fluids are known to the writers. The experimental data in reference [7] on "almost" straight cylinders are extensive, and they include flow induced curvature variations. The experimental 6061-T6 aluminum cylinder was characterized by eccentricity $e = 0.00139$, length 1.8 m, diameters 0.526 cm and 0.635 cm, and the fluid specific gravity was 0.986. With these data the numerical analysis of the in- and out-of-plane natural frequency-flow velocity relationship is determined as shown in Fig. 6. To correctly test the in-plane natural frequencies, the plane of the excitation must be coincident with the plane of principal curvature. Under these loading conditions the in- and out-of-plane response uncouple. In the experiments [7] the plane of excitation was "close" to the plane of principal curvature but not in it. The correspondence of the constant curvature results and the experiment is quite good. The constant curvature analysis provides a reasonably accurate procedure for predicting natural frequencies. Recall that the test cylinder was almost

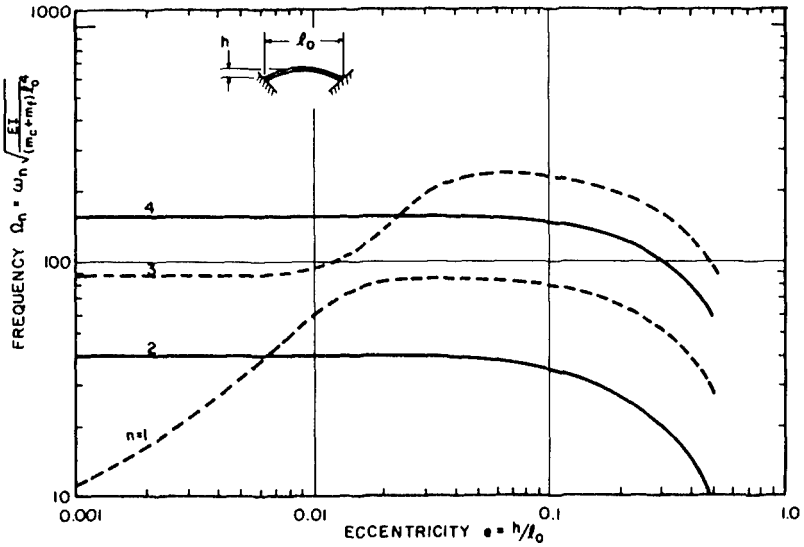

Fig. 4 Natural frequency for constant curvature ring sections of fixed chord length

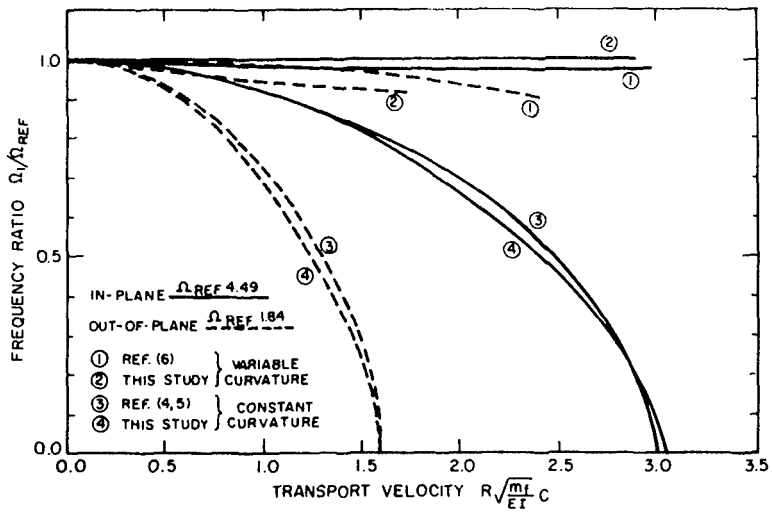

Fig. 5 In-plane and out-of-plane fundamental frequencies of a clamped semi-circular cylinder with mass transport

straight—e = 0.00139—so that the curved cylinder analysis becomes significant for small eccentricity or initial curvature.

A surprise in this analysis is the behavior of the in-plane, variable curvature, fundamental frequency that increases with transport velocity. The increase occurs because of 1 membrane tension, and 2 the fundamental frequency sensitivity to e illustrated in Fig. 4. For "almost" straight cylinders the fundamental frequency sensitivity to curvature is large and small e variations are significant. For large curvature, as in semicircular sections, the sensitivity of fundamental to e is small. While the variable curvature model possesses great intuitive appeal the natural frequency-transport velocity behavior is contrary to observation and possibly even contrary to expectation.

A precise explanation of the observed nonplanar response in [7] cannot be given because the curved geometry of the specimen was not satisfactorily recorded. From the original test model in which $\tau_0 = \kappa_0 = 0$ and $\kappa_0' = 1/R$, it is concluded that an uncoupled planar response is possible for excitation either in- or out-of-plane of principal curvature. However, in [7] the excitation was neither in nor out of that plane so a combined, orbital response was to be expected. This is thought to be the principal

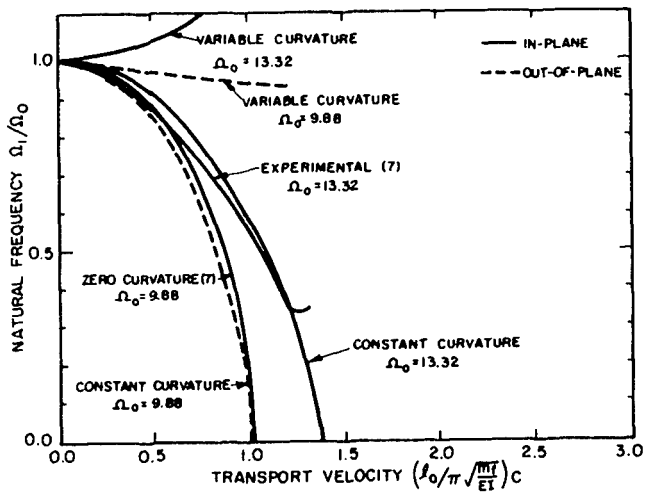

Fig. 6 Out-of-plane and in-plane fundamental frequency-transport velocity relationship for an "almost" straight, simply supported cylinder

cause of the observed motion. Variations in τ_0, κ_0, κ_0' as well as nonlinear contributions at the resonance amplitudes increases coupling although a quantitative evaluation of those effects is not possible.

Acknowledgments

The authors thank the National Science Foundation for financial support of this program. The authors also thank the University of California Forest Products Laboratory and the industrial sponsors for their continued and faithful support. The authors are also indebted to Ms. Sheila Slavin for her assistance with the preparation of the manuscript.

References

1 Paidoussis, M. P., and Issid, N. T., "Dynamic Stability of Pipes Conveying Fluid," *Journal of Sound and Vibration, 33*, 3, 1974, pp. 267–294.

2 Mote, C. D., Jr., "Dynamic Stability of Axially Moving Materials," feature article in the *Shock and Vibration Digest*, Vol. 4, No. 4, Apr. 1972.

3 Unny, T. E., Martin, E. L., and Dubey, R. N., "Hydroelastic Instability of Uniformly Curved Pipe-Fluid Systems," *Journal of Applied Mechanics*, TRANS. ASME, *37(3)*, 1970, pp. 817–822.

4 Chen, S. S., "Vibration and Stability of a Uniformly Curved Tube Conveying Fluid," *Journal of Acoustical Society of America, 51*, 1972, pp. 223–232.

5 Chen, S. S., "Out-of-Plane Vibration and Stability of Curved Tubes Conveying Fluid," *Journal of Applied Mechanics, 40(2)*, 1973, pp. 362–368.

6 Hill, J. L., and Davis, C. G., "The Effects of Initial Forces on the Hydroelastic Vibration and Stability of Planar Curved Tubes," *Journal of Applied Mechanics, 41(2)*, 1974, pp. 355–359.

7 Liu, H. S., and Mote, C. D., Jr., "Dynamic Response of Pipes Transporting Fluids," *Journal of Engineering for Industry*, TRANS. ASME, Vol. 96, Series B, 2, May 1974, pp. 591–596.

8 Love, A. E. H., *A Treatise on the Mathematical Theory of Elasticity*, Dover Publications, New York, 1966, pp. 444–454.

9 Tso, W. K., "On the Motion of a Curved and Twisted Rod," *ACTA Mechanica, 13*, 1972, pp. 163–178.

10 Doll, Robert W., and Mote, C. D., Jr., "The Dynamic Formulation and the Finite Element Analysis of Curved and Twisted Tubes Transporting Fluids," Report to the National Science Foundation, Dept. of Mechanical Engineering, Univ. of California, Berkeley, 1974.

11 Benjamin, T. B., "Dynamics of a System of Articulating Pipes Conveying Fluid, Parts I and II," *Proceedings of the Royal Society London*, Series *A*, *261*, 1961, pp. 457–499.

12 Goudreau, G. L., and Taylor, R. L., "Evaluation of Numerical Integration Methods in Elastodynamics," *Computer Methods in Applied Mechanics and Engineering, 2*, 1972, pp. 69–97.

13 Fried, I., "Accuracy and Condition of Curved (Isoparametric) Finite Elements," *Journal of Sound Vibration, 31(3)*, 1973, pp. 345–355.

14 Sabir, A. B., and Ashwell, D. G., "A Comparison of Curved Beam Finite Elements when Used in Vibration Problems," *Journal of Sound and Vibration, 18(4)*, 1971, pp. 555–563.

15 Archer, R. R., "Small Vibrations of Thin Incomplete Circular Rings," *International Journal of Mechanical Science, 1*, 1960, pp. 45–56.

16 Ojalvo, I. U., "Coupled Twist-Bending Vibrations of Incomplete Elastic Rings," *International Journal of Mechanical Science, 4*, 1962, pp. 53–72,

17 Leissa, Arthur W., "On a Curve Veering Aberration," ZAMP, Vol. 25, 1974, pp. 99–111.

18 Mote, C. D., Jr., and Matsumoto, G. Y., "Coupled Nonconservative Stability-Finite Element," *Journal of Engineering Mechanics*, ASCE, *EM3, 98*, 1972, pp. 595–608.

19 Chen, S. S., "Parallel Flow Induced Vibrations and Instabilities of Cylindrical Structures," *Shock & Vibration Digest*, Vol. 6, No. 10, Oct. 1974.

APPENDIX I

The elements of the $\underline{\alpha}$, $\underline{\beta}$ and $\underline{\gamma}$ operators are given here with the notation $D^k = d^k/ds^k$. All elements not included herein are zero.

$$\alpha_{11} = \alpha_{22} = \alpha_{33} = -(m_c + m_f) \tag{37}$$

$$\alpha_{44} = -I \tag{38}$$

$$\beta_{12} = -\beta_{21} = m_f c\kappa_0' \tag{39}$$

$$\beta_{13} = -\beta_{31} = m_f c\kappa_0 \tag{40}$$

$$\beta_{23} = -\beta_{32} = 2m_f c\tau_0 \tag{41}$$

$$\beta_{22} = \beta_{33} = -2m_f cD^1 \tag{42}$$

$$\begin{aligned}\gamma_{11} = {} & [EI_1\kappa_0^2 + EI_2\kappa_0'^2 + EA]D^2 + 2[EI_1\kappa_0\kappa_{0,s} + EI_2\kappa_0'\kappa_{0,s}']D^1 \\ & + [m_f c^2(\kappa_0^2 + \kappa_0'^2) - \kappa_0\tau_0\kappa_{0,s}'(EI_1 + EI_2) \\ & - \kappa_0\kappa_0'\tau_{0,s}(EI_1 - EI_2) + \kappa_0'\tau_0\kappa_{0,s}(EI_1 + EI_2) \\ & - \tau_0^2(\kappa_0'^2EI_1 + \kappa_0^2EI_2) + EI_1\kappa_0\kappa_{0,ss} + EI_2\kappa_0'\kappa_{0,ss}']\end{aligned} \tag{43}$$

$$\begin{aligned}\gamma_{12} = {} & EI_2\kappa_0'D^3 - \kappa_0\tau_0[2EI_1 + EI_2]D^2 + [m_f c^2\kappa_0' - 3EI_1\kappa_0\tau_{0,s} \\ & - \kappa_0'\tau_0(2EI_1 + EI_2) - \kappa_0'EA]D^1 + [-m_f c^2\kappa_0\tau_0 \\ & - EI_1\kappa_0\tau_{0,ss} + EI_2\kappa_0\tau_0^3 - \kappa_0'\tau_0\tau_{0,s}(EI_1 + 2EI_2) \\ & - \kappa_{0,s}'EA]\end{aligned} \tag{44}$$

$$\begin{aligned}\gamma_{13} = {} & -EI_1\kappa_0D^3 - \kappa_0'\tau_0[EI_1 + 2EI_2]D^2 + [-m_f c^2\kappa_0 \\ & - 3EI_2\kappa_2'\tau_{0,s} + \kappa_0\tau_0^2(EI_1 + 2EI_2) + \kappa_0EA]D^1 \\ & + [-m_f c^2\kappa_0'\tau_0 - EI_2\kappa_0'\tau_{0,ss} + EI_1\kappa_0'\tau_0^3 + \kappa_0\tau_0\tau_{0,s}(2EI_1 \\ & + EI_2) + \kappa_{0,s}EA]\end{aligned} \tag{45}$$

$$\begin{aligned}\gamma_{14} = {} & \kappa_0\kappa_0'[EI_1 - EI_2]D^1 + [\kappa_0'\kappa_{0,s}(EI_1 - EI_2) \\ & + \tau_0(EI_1\kappa_0'^2 + EI_2\kappa_0^2)]\end{aligned} \tag{46}$$

$$\begin{aligned}\gamma_{21} = {} & -EI_2\kappa_0'D^3 - [\tau_0\kappa_0(2EI_1 + EI_2) + 3EI_2\kappa_{0,s}']D^2 \\ & + [-m_f c^2\kappa_0' - 3EI_2\kappa_{0,ss}' - 2\tau_0\kappa_{0,s}(2EI_1 + EI_2) \\ & - \kappa_0\tau_{0,s}(EI_1 + 2EI_2) + \kappa_0'\tau_0^2(2EI_1 + EI_2) + \kappa_0'EA]D^1 \\ & + [-m_f c^2(\kappa_{0,s}' + \kappa_0\tau_0) + EI_1\tau_0(2\kappa_0'_{,s}\tau_0 + 3\kappa_0'\tau_{0,s}) \\ & - \kappa_{0,s}\tau_{0,s}(EI_1 + 2EI_2) - \tau_0\kappa_{0,ss}(2EI_1 + EI_2) + EI_2(\kappa_0\tau_0^3 \\ & + \tau_0^2\kappa_{0,s}' - \kappa_0\tau_{0,ss} - \kappa_{0,sss}')]\end{aligned} \tag{47}$$

$$\begin{aligned}\gamma_{22} = {} & -EI_2D^4 + [-m_f c^2 + 2\tau_0^2(2EI_1 + EI_2) + GJ\kappa_0^2]D^2 \\ & + 2[2\tau_0\tau_{0,s}(2EI_1 + EI_2) + GJ\kappa_0\kappa_{0,s}]D^1 \\ & + [m_f c^2\tau_0^2 - EI_2\tau_0^4 + \tau_{0,s}^2(EI_1 + 2EI_2) \\ & + 2\tau_0\tau_{0,ss}(EI_1 + EI_2) + GJ(-\kappa_0'^2\tau_0^2 \\ & + \kappa_0\kappa_0'\tau_{0,s} + \kappa_0\tau_0\kappa_{0,s}' + \tau_0\kappa_{0,s}) - \kappa_0'^2EA]\end{aligned} \tag{48}$$

$$\begin{aligned}\gamma_{23} = {} & 2\tau_0[EI_1 + EI_2]D^3 + [\tau_{0,s}(EI_1 + 5EI_2) + GJ\kappa_0\kappa_0']D^2 \\ & + [2m_f c^2\tau_0 + 4EI_2\tau_{0,ss} - 2\tau_0^3(EI_1 + EI_2) \\ & + GJ(\kappa_0\kappa_{0,s}' + \kappa_0'\kappa_{0,s} - \kappa_0'^2\tau_0 - \kappa_0^2\tau_0]D^1 \\ & + [m_f c^2\tau_{0,s} + EI_2\tau_{0,sss} - \tau_0^2\tau_{0,s}(5EI_1 + EI_2) \\ & + GJ(\kappa_0\kappa_0'\tau_0^2 - \kappa_0^2\tau_{0,s} - 2\kappa_0\tau_0\kappa_{0,s}) + \kappa_0\kappa_0'EA]\end{aligned} \tag{49}$$

$$\begin{aligned}\gamma_{24} = {} & \kappa_0[EI_2 + GJ]D^2 + [-\kappa_0'\tau_0(2EI_1 + GJ) \\ & + \kappa_{0,s}(2EI_2 + GJ)]D^1 \\ & + [-EI_1(2\tau_0\kappa_{0,s}' + \kappa_0'\tau_{0,s}) \\ & + EI_2(\kappa_{0,ss} - \kappa_0\tau_0^2)]\end{aligned} \tag{50}$$

$$\begin{aligned}\gamma_{31} = {} & EI_1\kappa_0D^3 + [-\kappa_0'\tau_0(EI_1 + 2EI_2) + 3EI_1\kappa_{0,s}]D^2 \\ & + [m_f c^2\kappa_0 + 3EI_1\kappa_{0,ss} - 2\tau_0\kappa_{0,s}'(EI_1 + 2EI_2) \\ & - \kappa_0'\tau_{0,s}(2EI_1 + EI_2) - \kappa_0\tau_0^2(EI_1 + 2EI_2) \\ & - \kappa_0EA]D^1 + [m_f c^2(-\kappa_0'\tau_0 + \kappa_{0,s}) \\ & - \tau_0\kappa_{0,ss}'(EI_1 + 2EI_2) - \kappa_{0,s}'\tau_{0,s}(2EI_1 + EI_2)\end{aligned}$$

$$+ EI(\kappa_{0,sss} - \kappa_0'\tau_{0,ss} - \kappa_{0,s}\tau_0^2 + \kappa_0'\tau_0^3)$$
$$- EI_2\tau_0(2\tau_0\kappa_{0,s} + 3\kappa_0\tau_{0,s})] \quad (51)$$

$$\gamma_{32} = 2\tau_0[EI_1 + EI_2]D^3 + [-\tau_{0,s}(5EI_1 + EI_2) + GJ\kappa_0\kappa_0']D^2$$
$$+ [-2m_fc^2\tau_0 - 4EI_1\tau_{0,ss} + 2\tau_0^3(EI_1 + EI_2)$$
$$+ GJ(\kappa_0'\kappa_{0,s} + \kappa_0\kappa_{0,s}' + \kappa_0'^2\tau_0 + \kappa_0^2\tau_0]D^1$$
$$+ [-m_fc^2\tau_{0,s} - EI_1\tau_{0,sss} + \tau_0^2\tau_{0,s}(EI_1 + 5EI_2)$$
$$+ GJ(2\kappa_0'\tau_0\kappa_{0,s}' + \kappa_0'\tau_{0,s} + \kappa_0\kappa_0'\tau_0^2) + \kappa_0\kappa_0'EA] \quad (52)$$

$$\gamma_{33} = -EI_1D^4 + [-m_fc^2 + 2\tau_0^2(EI_1 + 2EI_2) + GJ\kappa_0'^2]D^2$$
$$+ 2[2\tau_0\tau_{0,s}(EI_1 + 2EI_2) + GJ\kappa_0'\kappa_{0,s}']D^1 + [m_fc^2\tau_0^2$$
$$- EI_1\tau_0^4 + \tau_{0,s}^2(2EI_1 + EI_2) + 2\tau_0\tau_{0,ss}(EI_1 + EI_2)$$
$$- GJ(\kappa_0'\tau_0\kappa_{0,s} + \kappa_0\tau_0\kappa_{0,s}' + \kappa_0\kappa_0'\tau_{0,s} + \kappa_0^2\tau_0^2) - EA\kappa_0^2 \quad (53)$$

$$\gamma_{34} = \kappa_0'[EI_1 + GJ]D^2 + [\kappa_{0,s}'(2EI_1 + GJ) + \kappa_0\tau_0(2EI_2$$
$$+ GJ)]D^1 + [EI_1(\kappa_{0,ss}' - \kappa_0'\tau_0^2) + EI_2(2\tau_0\kappa_{0,s} + \kappa_0\tau_{0,s})] \quad (54)$$

$$\gamma_{41} = -\kappa_0\kappa_0'[EI_1 - EI_2]D^1 + [\tau_0(EI_1\kappa_0'^2 + EI_2\kappa_0^2)$$
$$+ EI_1(\kappa_0\kappa_{0,s}' - \kappa_0'\kappa_{0,s})] \quad (55)$$

$$\gamma_{42} = \kappa_0[EI_2 + GJ]D^2 + [\kappa_0'\tau_0(2EI_1 + GJ) + GJ\kappa_{0,s}]D^1$$
$$+ [\kappa_0'\tau_{0,s}(EI_1 + GJ) - EI_2\kappa_0\tau_0^2 + GJ\kappa_{0,s}'\tau_0] \quad (56)$$

$$\gamma_{43} = \kappa_0'[EI_1 + GJ]D^2 + [-\kappa_0\tau_0(2EI_2 + GJ) + GJ\kappa_{0,s}']D^1$$
$$- [\kappa_0\tau_{0,s}(EI_2 + GJ) + EI_1\kappa_0'\tau_0^2 + GJ\kappa_{0,s}\tau_0]$$

$$\gamma_{44} = GJD^2 - [EI_1\kappa_0'^2 + EI_2\kappa_0^2]$$

Table 1 Boundary conditions

Clamped	Pinned	Free
$\delta w = 0$	$\delta w = 0$	$A_1w_{,s} + A_2w - EI_2\kappa_0'u_{,ss} + 2EI_2\kappa_0\tau_0u_{,s} + A_3u + EI_1\kappa_0v_{,ss} + 2EI_2\kappa_0'\tau_0v_{,s} + A_4v + A_5\theta - m_fcw_{,t} = m_fc^2$
$\delta u = 0$	$\delta u = 0$	$EI_2\kappa_0'w_{,ss} + B_1w_{,s} + B_2w + m_fcu_{,t} + EI_2u_{,sss} + B_3u_{,s} + B_4u + B_5v_{,ss} + B_6v_{,s} + B_7v + B_8\theta_{,s} + B_9\theta - m_fc[u_{,t} + c(u_{,s} - \tau_0v + \kappa_0'w)] = 0$
$\delta u_{,s} = 0$	$-EI_2[u_{,ss} - \tau_0^2u - 2\tau_0v_{,s} - \tau_{0,s}v + \kappa_0'w_{,s} + (\kappa_0\tau_0 + \kappa_{0,s}')w - \kappa_0\theta] = 0$	$-EI_2[u_{,ss} - \tau_0^2u - 2\tau_0v_{,s} - \tau_{0,s}v + \kappa_0'w_{,s} + (\kappa_0\tau_0 + \kappa_{0,s}')w - \kappa_0\theta] = 0$
$\delta v = 0$	$\delta v = 0$	$-EI_1\kappa_0w_{,ss} + C_1w_{,s} + C_2w + C_3u_{,ss} + C_4u_{,s} + C_5u + m_fcv_{,t} + EI_1v_{,sss} + C_6v_{,s} + C_7v + C_8\theta_{,s} + C_9\theta - m_fc[v_{,t} + c(v_{,s} + \tau_0u - \kappa_0w)] = 0$
$\delta v_{,s} = 0$	$-EI_1[2\tau_0u_{,s} + \tau_{0,s}u + v_{,ss} - \tau_0^2v - \kappa_0w_{,s} + (\kappa_0'\tau_0 - \kappa_{0,s})w - \kappa_0'\theta = 0$	$-EI_1[2\tau_0u_{,s} + \tau_{0,s}u + v_{,ss} - \tau_0^2v - \kappa_0w_{,s} + (\kappa_0'\tau_0 - \kappa_{0,s})w - \kappa_0'\theta] = 0$
$\delta\theta = 0$	$\delta\theta = 0$	$-GJ[\kappa_0u_{,s} + \kappa_0'\tau_0u + \kappa_0'v_{,s} - \kappa_0\tau_0v + \theta_{,s}] = 0$

$$A_1 = -EI_1\kappa_0^2 - EI_2\kappa_0'^2 - EA$$
$$A_2 = \kappa_0\kappa_0'\tau_0(EI_1 - EI_2) - EI_1\kappa_0\kappa_{0,s} - EI_2\kappa_0'\kappa_{0,s}'$$
$$A_3 = EI_1\kappa_0\tau_{0,s} + EI_2\kappa_0'\tau_0^2 + \kappa_0'EA$$
$$A_4 = -EI_1\kappa_0\tau_0^2 + EI_2\kappa_0'\tau_{0,s} - \kappa_0EA$$
$$A_5 = -\kappa_0\kappa_0'(EI_1 - EI_2)$$
$$B_1 = 2EI_2\kappa_{0,s}' + \kappa_0\tau_0(2EI_1 + EI_2)$$
$$B_2 = m_fc^2\kappa_0' + \tau_0\kappa_{0,s}(2EI_1 + EI_2) - 2EI_1\kappa_0'\tau_0^2 + EI_1\kappa_{0,ss}' + EI_2\kappa_0\tau_{0,s}$$
$$B_3 = m_fc^2 - \tau_0^2(4EI_1 + EI_2) - GJ\kappa_0^2$$
$$B_4 = -2\tau_0\tau_{0,s}(EI_1 + EI_2) - GJ\kappa_0\kappa_0'\tau_0$$
$$B_5 = -2\tau_0(EI_1 + EI_2)$$
$$B_6 = -3EI_1\tau_{0,s} - GJ\kappa_0\kappa_0'$$
$$B_7 = -m_fc^2\tau_0 + 2EI_1\tau_0^3 - EI_2\tau_{0,ss} + GJ\kappa_0^2\tau_0$$
$$B_8 = -\kappa_0(EI_2 + GJ)$$
$$B_9 = 2EI_1\kappa_0'\tau_0 - EI_2\kappa_{0,s}$$

and

$$C_1 = -2EI_1\kappa_{0,s} + \kappa_0'\tau_0(EI_1 + 2EI_2)$$
$$C_2 = -m_fc^2\kappa_0 + EI_1(\kappa_0'\tau_{0,s} - \kappa_{0,ss}) + \tau_0\kappa_{0,s}'(EI_1 + 2EI_2) + 2EI_2\kappa_0\tau_0^2$$
$$C_3 = 2\tau_0(EI_1 + EI_2)$$
$$C_4 = 3EI_1\tau_{0,s} - GJ\kappa_0\kappa_0'$$
$$C_5 = m_fc^2\tau_0 + EI_1\tau_{0,ss} - 2EI_2\tau_0^3 - GJ\kappa_0'\tau_0$$
$$C_6 = m_fc^2 - \tau_0^2(EI_1 + 4EI_2) - GJ\kappa_0'^2$$
$$C_7 = -2\tau_0\tau_{0,s}(EI_1 + EI_2) + GJ\kappa_0\kappa_0'\tau_0$$
$$C_8 = -\kappa_0'(EI_1 + GJ)$$
$$C_9 = -EI_1\kappa_{0,s}' - 2EI_2\kappa_0\tau_0$$